THE JOURNAL OF BIOLOGICAL CHEMISTRY VOL. 286, NO. 12, pp. 10169–10176, March 25, 2011

Halotolerant Cyanobacterium *Aphanothece halophytica* Contains an Na^+-dependent F_1F_0-ATP Synthase with a Potential Role in Salt-stress Tolerance*[S]

Received for publication, December 2, 2010, and in revised form, January 20, 2011 Published, JBC Papers in Press, January 24, 2011, DOI 10.1074/jbc.M110.208892

Kanteera Soontharapirakkul[‡§], Worrawat Promden[‡], Nana Yamada[‡], Hakuto Kageyama[‡], Aran Incharoensakdi[§], Atsuko Iwamoto-Kihara[¶], and Teruhiro Takabe[‡‖1]

From the [‡]Graduate School of Environmental and Human Sciences, Meijo University, Nagoya 468-8502, Japan, the [§]Faculty of Sciences, Chulalongkorn University, Patumwan, Bangkok 10330, Thailand, the [¶]Faculty of Bioscience, Nagahama Institute of Bio-science and Technology, Shiga, Nagahama 526-0829, Japan, and the [‖]Research Institute, Meijo University, Nagoya 468-8502, Japan

Aphanothece halophytica **is a halotolerant alkaliphilic cyanobacterium that can grow in media of up to 3.0 M NaCl and pH 11. Here, we show that in addition to a typical H^+-ATP synthase, *Aphanothece halophytica* contains a putative F_1F_0-type Na^+-ATP synthase ($ApNa^+$-ATPase) operon (*$ApNa^+$-atp*). The operon consists of nine genes organized in the order of putative subunits *β*, *ϵ*, I, hypothetical protein, a, c, b, *α*, and *γ*. Homologous operons could also be found in some cyanobacteria such as *Synechococcus* sp. PCC 7002 and *Acaryochloris marina* MBIC11017. The *$ApNa^+$-atp* operon was isolated from the *A. halophytica* genome and transferred into an *Escherichia coli* mutant DK8 (Δ*atp*) deficient in ATP synthase. The inverted membrane vesicles of *E. coli* DK8 expressing $ApNa^+$-ATPase exhibited Na^+-dependent ATP hydrolysis activity, which was inhibited by monensin and tributyltin chloride, but not by the protonophore, carbonyl cyanide *m*-chlorophenyl hydrazone (CCCP). The Na^+ ion protected the inhibition of $ApNa^+$-ATPase by *N,N′*-dicyclohexylcarbodiimide. The ATP synthesis activity was also observed using the Na^+-loaded inverted membrane vesicles. Expression of the *$ApNa^+$-atp* operon in the heterologous cyanobacterium *Synechococcus* sp. PCC 7942 showed its localization in the cytoplasmic membrane fractions and increased tolerance to salt stress. These results indicate that *A. halophytica* has additional Na^+-dependent F_1F_0-ATPase in the cytoplasmic membrane playing a potential role in salt-stress tolerance.**

The F_1F_0-type ATP synthase (ATPase) plays vital functions in the energy-transducing membranes of bacteria, mitochondria, and chloroplasts by catalyzing ATP synthesis and hydrolysis coupled with transmembrane proton or sodium ion transport (1). The hydrophilic extramembranous F_1 domain consists of five different polypeptides with a stoichiometry of $\alpha_3\beta_3\gamma\delta\epsilon$. The integral membrane F_0 domain consists of three different polypeptides (a, b, and c) and mediates the transfer of protons or sodium ions across the membrane. The number of c subunits shows substantial variation in different organisms (2). Like F_1F_0-type ATPases, vacuolar V_1V_0- and archaea A_1A_0-type ATPases are also membrane-anchored rotary enzymes, although former functions primarily as an ATP-driven ion pump (1, 3).

Plants are known to have two F-type ATPases, one each in the chloroplast and mitochondria, and one V-type ATPase residing in the vacuole. The cyanobacteria are oxygenic photosynthetic organisms and possess one F-type ATPase in the thylakoid membranes. All of these complexes use proton as the coupling ion (1–3).

To survive at high salinity, living organisms must prevent the excessive Na^+ accumulation in the cytoplasm. To date, two types of Na^+-transporting mechanisms are known to extrude Na^+ from the cytoplasm. The Na^+/H^+ antiporters are of one type that utilize energy of the transmembrane proton gradient for Na^+ translocation (4), whereas another type is the primary ATP-driven Na^+-pumps in the plasma membrane (P-type Na^+-ATPase) (5, 6). The P-type Na^+-ATPase is a single component polypeptide found in many organisms, including yeast. However, the presence of P-type Na^+-ATPase in plants and algae seems to be rare.

Aphanothece halophytica is a halotolerant cyanobacterium isolated from the Dead Sea. *A. halophytica* is known to accumulate betaine and can grow in a wide range of salinity (0.25–3.0 M NaCl) as well as at alkaline pH conditions (7). Previous studies have shown that *A. halophytica* has a unique biosynthetic pathway of osmoprotectant betaine consisting of three-step methylation of glycine (8) and novel Na^+/H^+ antiporters such as Ap-NhaP1, Ap-NapA1–1, Ap-NapA1–2, and Ap-Mrp (9–11). From the shotgun sequencing of the whole genome, we found that *A. halophytica* contains a putative F_1F_0-type Na^+-ATP synthase ($ApNa^+$-ATPase) operon (*$ApNa^+$-atp*). Isolation of the operon and its functional characterization are described below.

EXPERIMENTAL PROCEDURES

Strains and Culture Conditions—A. halophytica cells were grown photoautotrophically in the BG11 liquid medium con-

* This work was supported in part by grants-in-aid for scientific research from the Ministry of Education, Science, and Culture of Japan; the Salt Science Research Foundation; and the High-Technology Research Center of Meijo University. This work was also supported by the Royal Golden Jubilee Ph.D. program and the 90th Anniversary of Chulalongkorn University Fund (Ratchadaphiseksomphote Endowment Fund) (to K. S.).

[S] The on-line version of this article (available at http://www.jbc.org) contains supplemental Figs. S1 and S2.

[1] To whom correspondence should be addressed: 1-501 Shiogamaguchi, Tenpaku-ku, Nagoya, Aichi 468-8502, Japan. Fax: 81-52-832-1545; E-mail: takabe@meijo-u.ac.jp.

taining 18 mM $NaNO_3$ and Turk Island salt solution at 30 °C (7, 12). *Synechococcus* sp. strain PCC 7942 cells were also grown in the BG11 liquid medium supplemented with 10 mM HEPES-KOH and bubbled with 3% CO_2 at 30 °C under continuous fluorescent white light (40 μE m^{-2} s^{-1}). *Escherichia coli* DH5α and DK8 (Δ*atp*) (13) cells were grown at 37 °C in Luria-Bertani (LB) medium.

Construction of Expression Plasmids—The *ApNa*$^+$*-atp* operon of *A. halophytica* was amplified by PCR using the primer set ApATPaseBamHI-F/ApATPaseSalI-R. The sequences of ApATPaseBamHI-F and ApATPaseSalI-R are 5′-GGATCC-GGAGTTAGGGGCGATGGTACAAT-3′ and 5′-GTCGAC-GGATGAAGGATGATCACTC-3′, respectively. The amplified fragment was ligated into the EcoRV site of pBSK+ (Stratagene) and sequenced. The insert was then cloned in frame into the BamHI/SalI sites of pTrcHis2C (Invitrogen) with the C-terminal peptide of His_6 tag. The resulting plasmid, pTrcHis2C-*ApNa*$^+$*-atp* was introduced first to *E. coli* DH5α and then to DK8 cells (13).

Complementation Tests—For the complementation test, *E. coli* DK8 cells transformed with pTrcHis2C or pTrcHis2C-*ApNa*$^+$*-atp* were grown overnight in LB medium at 37 °C. Cells were plated on to a 1.5% M13 minimal medium agar plate (pH 7.0), containing 42 mM Na_2HPO_4, 22 mM KH_2PO_4, 8.5 mM NaCl, 2 mM $MgSO_4$, 0.1 mM $CaCl_2$, 15 μM thiamine, a carbon source (35 mM glucose or 35 mM succinate), and 1 mM isopropyl-β-D-thiogalactopyranoside. Plates were incubated at 37 °C for 2 days. For growth experiments, the *E. coli* DK8 cells grown in LB medium at the late logarithmic phase were transferred into fresh medium containing various concentrations of NaCl at pH 7.0 with a starting A_{620} of 0.02.

Preparation of Inverted (Inside Out) Membrane Vesicles from E. coli DK8—Cells were harvested at exponential growth phase and washed with 20 mM Tris-HCl (pH 7.6) containing 1.0 M sucrose. The collected cells were resuspended in extraction buffer (20 mM Tris-HCl, pH 7.6, 1 mM DTT, 1 mM PMSF, and 5 mM $MgCl_2$) with a ratio (g ml^{-1}) of 1.0:2.0. After homogenization, cells were disrupted by two passages through a French pressure cell at 400 kilopascals. Unbroken cells and large debris were removed by centrifugation at 4000 × *g* for 15 min. The inverted membrane vesicles were sedimented by centrifugation at 100,000 × *g* for 30 min and resuspended in 50 mM HEPES-KOH, pH 7.0, to a final protein concentration of 1 mg ml^{-1}.

Determination of ATPase Hydrolysis Activity—The ATPase activity was assayed by measuring the release of inorganic phosphate resulting from the hydrolysis of ATP. The reaction mixture (1 ml) contained 20 mM Tris-HCl, pH 7.6, 5 mM $MgCl_2$, 10 mM NaCl, and membrane vesicles (30 μg of protein). The reaction was started by addition 4 mM ATP (Tris salt).

Preparation of Na^+-loaded Membrane Vesicles—Inverted membrane vesicles were prepared in 5 mM potassium phosphate, pH 7.5, containing 0.25 mM EDTA and 0.2 M NaCl. After incubation for 1 day, Na^+-loaded membrane vesicles were collected by centrifugation at 100,000 × *g* for 1 h and resuspended again in 5 mM potassium phosphate, pH 7.5, containing 0.25 M EDTA.

Determination of ATP Synthesis—ATP synthesis was measured in the reaction medium (0.5 ml) containing 5 mM potassium phosphate, pH 7.5, 5 mM $MgCl_2$, 0.2 M KCl, 0.1 mM ADP, 1 μM valinomycin, and Na^+-loaded-membrane vesicles (30 μg protein). At different time intervals, 50-μl sample was taken out and added immediately to 5 μl of 20% TCA. The samples were then centrifuged at 13,000 × *g* for 5 min. Aliquot (1 μl) of the supernatant was diluted with 99 μl of distilled water, and the ATP content was determined by luciferin/luciferase reaction.

Expression of ApNa$^+$*-atp Operon in the Heterologous Freshwater Cyanobacterium Synechococcus sp. PCC 7942*—The pTrcHis2C-*ApNa*$^+$*-atp,* which contains the *trc* promoter, was digested with ScaI and then ligated into the *E. coli*/*Synechococcus* shuttle vector pUC303 at the SalI-digested and blunt-ended site. The resulting plasmid, designated as pUC303-*ApNa*$^+$*-atp*, was used to transform *Synechococcus* sp. strain PCC 7942 cells (10). For salt stress experiments, *Synechococcus* cells were subcultured in BG11 medium as described above but supplemented with 50 μg ml^{-1} streptomycin. Cells at the late logarithmic phase were transferred into fresh medium containing various concentrations of NaCl (0–0.5 M). The isopropyl-β-D-thiogalactopyranoside (0.5 mM) was used to induce the *ApNa*$^+$*-atp* expression under the *trc* promoter.

Preparation of Inverted Membrane Vesicles from Synechococcus sp. PCC 7942—Cells were harvested at exponential growth phase and washed with 20 mM Tris-HCl, pH 7.6, containing 1.0 M sucrose. The collected cells were resuspended in extraction buffer (20 mM Tris-HCl, pH 7.6, 1 mM DTT, 1 mM PMSF, and 5 mM $MgCl_2$) with a ratio (g ml^{-1}) of 1.0:2.0. After homogenization, the cells were disrupted by two passages through a French pressure cell at 400 kilopascals. Unbroken cells and large debris were removed by centrifugation at 9800 × *g* for 15 min. The inverted membrane vesicles were sedimented by centrifugation at 100,000 × *g* for 30 min and resuspended in 50 mM HEPES-KOH, pH 7.0, to a final protein concentration of 1 mg ml^{-1}.

Isolation of Thylakoid and Cytoplasmic Membranes from Synechococcus sp. PCC 7942—The above prepared membrane vesicles (total membrane fraction) were used for the separation of thylakoid and cytoplasmic membranes by sucrose gradient centrifugation at 110,000 × *g* for 16 h (14). The gradient consisted of four layers: 5.5 ml of 58% sucrose, 4.5 ml of 40% sucrose, 4.5 ml of 30% sucrose, and 4 ml of 10% sucrose layer. Thylakoid membranes remained at the 40/58% sucrose interphase, whereas cytoplasmic membranes moved into the 30% sucrose layer that was essentially free of chlorophyll (14).

Other Methods—The nucleotide sequences were determined using an ABI310 genetic analyzer (Applied Biosystems, Foster City, CA). Cellular ions were determined with a Shimadzu PIA-1000 personal ion analyzer (9). Protein concentration was measured using the Bradford's method. SDS-PAGE and Western blot analysis were carried out as described previously (15). Antibody raised against the His_6 tag was obtained from R&D Systems (Minneapolis, MN).

Nucleotide Sequence Accession Number—Nucleotide sequence data of the *ApNa*$^+$*-atp* operon from *A. halophytica* are deposited to the DDBJ database under the accession nos. AB602793, AB602794, and AB602795.

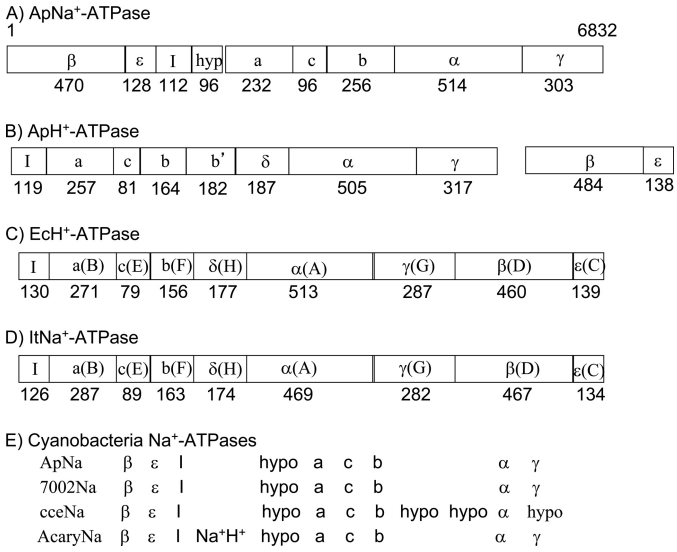

FIGURE 1. **Schematic structures of gene organization of several ATP synthases.** *A*, ApNa$^+$-ATPase (accession no. AB602793); *B*, ApH$^+$-ATPase (AB602794, AB602795); *C*, EcH$^+$-ATPase (*E. coli*, J01594); *D*, ItNa$^+$-ATPase (*I. tartaricus*, AF522463); and *E*, four kinds of cyanobacterial Na$^+$-ATPases. In *A*, *B*, and *E*, names of encoded proteins are shown. In *C* and *D*, both genes and encoded-proteins are shown. In *E*, ApNa, 7002Na, cceNa, and AcaryNa show the putative Na$^+$-ATPases from *A. halophytica* (AB602793), *Synechococcus* sp. PCC7002 (SYNPCC7002_G0144–0152), *Cyanothece* sp. ATCC 51142 (cce_1502–1512), and *A. marina* (AM1_D0157–0165), respectively. The numbers of amino acid residues in each subunit are shown *below* the *boxes*.

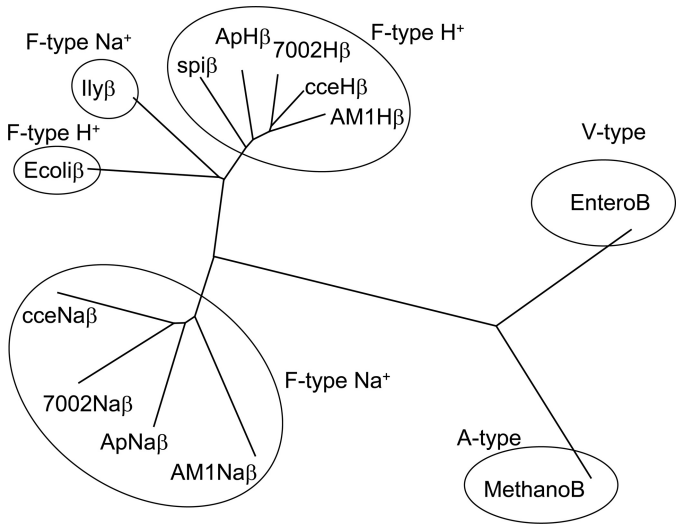

FIGURE 2. **Phylogenetic trees for β subunit of H$^+$- and Na$^+$-translocating ATPases from several species.** F-type Na$^+$ translocating β subunits, AB602793 (*ApNaβ*), cce_1512 (*cceNaβ*), SYNPCC7002_G0144 (*7002Naβ*), AM1_D0157 (*AM1Naβ*), and AF522463 (*IlyNaβ*). F-type H$^+$ translocating β subunits, AB602795 (*ApHβ*), cce_1512 (*cceHβ*), SYNPCC7002_G0144 (*7002Hβ*), AM1_D0157 (*AM1Hβ*), and spinach β subunit (*spiβ*, NP_054943). An A-type β subunit of *Methanosarcina mazei*, MetanoB (NP_632803.1) and V-type β subunit of *Enterococcus faecalis*, EnteroB (NP_815220.1) are shown.

RESULTS

Gene Organization in ApNa$^+$-atp Operon of A. halophytica—From the shotgun sequence analysis of the *A. halophytica* genome, we found a putative F_1F_0-type *ApNa$^+$-atp* operon in addition to the typical H$^+$-ATPase (ApH$^+$-ATPase) operon (*ApH$^+$-atp*). The *ApNa$^+$-atp* operon had nine ORFs, each with a putative start codon. These genes were organized in the order *atpD* (β), *atpC* (ϵ), *atpI* (I), hypothetical gene (*hyp*), *atpB* (a), *atpE* (c), *atp F* (b), *atpA* (α), *and atp G* (γ) (Fig. 1*A*). By contrast, gene organization of *ApH$^+$-atp* splits into two clusters, encoding Iacbb′δαγ and βϵ (Fig. 1*B*). The gene organization of *ApNa$^+$-atp* is similar to those of the *atp* operons in *E. coli* (*EcH$^+$-atp*) (13, 16) and *Ilyobacter tartaricus* (*ItNa$^+$-atp*) (16) that encode F-type H$^+$- and Na$^+$-ATPases, respectively. But, in *EcH$^+$-atp* and *ItNa$^+$-atp*, the operon starts from gene I and does not contain the hypothetical gene (Fig. 1, *C* and *D*). A Blast search revealed the presence of a similar operon in some cyanobacteria, such as *Synechococcus* sp. PCC 7002, *Acaryochloris marina* MBIC11017, and *Cyanothece* sp. ATCC 51142 (Fig. 1*E*). Among them, *Synechococcus* sp. PCC 7002 had the same gene organization to that of *ApNa$^+$-atp*, whereas in *A. marina* MBIC11017 and *Cyanothece* sp. ATCC 51142, additional gene(s) were found.

The deduced protein sequences of the nine genes, except the gene encoding hypothetical protein, were compared with the corresponding sequences of ATPase subunits from different species. The protein encoded by *ApNa$^+$-atpI* showed the least homologous (4–7% identity) compared with the corresponding subunit of H$^+$-transporting ATPase from *E. coli* and Na$^+$-transporting ATPase from *I. tartaricus*, *Propionigenium modestum*, *Acetobacterium woodii*, and *Clostridium paradoxum*. The α and β subunits of ApNa$^+$-ATPase showed greater similarity to the corresponding subunits from other species (40–51% identity) than the remaining subunits, which showed ~15–39% identity.

β Subunit of ApNa$^+$-ATPase Exhibits Higher Homology to Those of ItNa$^+$-ATPase and EcH$^+$-ATPase than That of ApH$^+$-ATPase—Fig. 2 shows the phylogenetic tree of several ATPases. The β subunit of ApH$^+$-ATPase exhibited high homology to the cyanobacterial H$^+$-ATPases from *Synechococcus* sp. PCC 7002, *A. marina* MBIC11017, and *Cyanothece* sp. ATCC 51142. It also exhibited high homology to that of spinach H$^+$-ATPase, supporting the view that the plant chloroplast originated through endosymbiosis from a cyanobacterium. The β subunit of ApNa$^+$-ATPase exhibited high homology to the Na$^+$-ATPases from *Synechococcus* sp. PCC 7002, *A. marina* MBIC11017, and *Cyanothece* sp. ATCC 51142, but relatively low homology to subunit B of A-type ATPase from *Methanosarcina mazei* Go1 and V-type ATPase from *Enterococcus hirae*. This result suggests that cyanobacterial Na$^+$-ATPases are F-type ATPase, and evolved earlier than the separation between cyanobacteria, *E. coli*, and *I. tartaricus*.

ApNa$^+$-ATPase Has Putative Na$^+$-binding Site in Subunit c—The membrane-spanning helices of the multiple copies of subunit c in the F_0 complex are the rotor ring of H$^+$ (or Na$^+$)-translocating ATP synthases (1). Supplemental Fig. S1*A* shows the phylogenetic tree of subunit c in several ATPases. Subunit c of ApH$^+$-ATPase exhibited high homology to that of cyanobacterial H$^+$-ATPase and spinach H$^+$-ATPase but was considerably different from that of ApNa$^+$-ATPase, which is similar to the phylogenic tree of β subunit. Supplemental Fig. S1*B* shows the alignment of subunit c of several F-type ATPases. Based on x-ray crystallography, cryo-electron microscopy, and atomic force microscopy studies, the binding sites for H$^+$ and Na$^+$ have been identified (1, 17). The binding site of H$^+$ in subunit c in spinach H$^+$-ATPase has been assigned as Gln (Gln-34, num-

bering in subunit c of $ApNa^+$-ATPase, Phe (Phe-65), Glu (Glu-67), Thr (Thr-70), and Tyr (Tyr-72), whereas the binding site of Na^+ in subunit c of $ItNa^+$-ATPase has been assigned as Gln (Gln-34), Val (Val-65), Glu (Glu-67), Ser (Ser-68), and Tyr (Tyr-72). The H^+-binding site (Gln-34, Phe-65, Glu-67, Thr-70, and Tyr-72) was conserved in all cyanobacterial H^+-translocating ATPases (supplemental Fig. S1*B*). For the Na^+-binding site, Glu-67, Ser-68, and Tyr-72 were conserved in all cyanobacterial Na^+-translocating ATPases. However, the Gln-34 changed to Glu (Glu-34) in all cyanobacterial Na^+-ATPases. Val-65 did not change, but Glu-67, Ser-68, and Thr-69 motif were conserved. These results indicate that ApH^+-ATPase presumably H^+-translocating ATPases, although ion specificity of $ApNa^+$-ATPase need to be tested experimentally.

$ApNa^+$-ATPase and ApH^+-ATPase Do Not Have Cys Residues Involved in Redox-induced Activation of Plant ATPase—The plant F-type H^+-ATPase has a unique regulatory mechanism, which is caused by a redox change of two cysteine residues located in the γ subunit. Under light, the reducing equivalents produced by photosynthetic electron transport reduce thioredoxin, which in turn reduces the disulfide bond formed within the γ subunit, yielding the active enzyme. The two cysteine residues forming the disulfide bond in the spinach H^+-ATPase were assigned to Cys-199 and Cys-205 (18). Supplemental Fig. S2*A* shows the alignment of the γ subunit of several F-type ATPases. Cys-199 and Cys-205 of spinach H^+-ATPase are shown in supplemental Fig. S2*A* in *closed boxes*. These cysteines were not conserved in all F-type ATPases from cyanobacteria, *E. coli*, and *I. tartaricus.* The spinach γ subunit is unique in having an extra domain around the two cysteine residues as shown by the *dotted line box*. In the cyanobacterial H^+-ATPase, the extradomain was nine residues smaller and did not contain the two cysteine residues. By contrast, in the cyanobacterial Na^+-ATPase, that type of extradomain was missing as is the case also in *E. coli* and *I. tartaricus.* The phylogenetic tree in supplemental Fig. S2*B* showed that the γ subunit of spinach H^+-ATPase was separated from that of cyanobacterial H^+-ATPase, indicating the evolution of unique regulating system in plant H^+-ATP synthetases.

Cloning of $ApNa^+$-atp and Expression in E. coli DK8 Cells—To clone the *$ApNa^+$-atp* operon from *A. halophytica*, PCR amplification was performed resulting in a 6832-bp PCR product in which the GTG start codon in *atpD* was changed to ATG. The PCR product was cloned into the EcoRV restriction site of pBSK+ vector and sequenced. Although one nucleotide change from GAG (Glu-41) to GAT (Asp-41) was found in the β subunit, this clone was used for further experiments because the substitution is rather conserved. Then, the insert was digested with BamHI and SalI and subcloned into the BamHI/SalI sites of pTrcHis2C expression vector. The last gene, *atpG*, was fused in frame with His_6 tag.

To examine the functional properties of *$ApNa^+$-atp*, these genes were expressed in the *E. coli* mutant DK8 lacking the *unc* operon encoding ATPase (Δ*atp*). As shown in Fig. 3*A*, the γ subunit of $ApNa^+$-ATPase could be detected in the *E. coli* DK8 cells transformed with pTrcHis2C-*$ApNa^+$-atp* but not with the vector alone. The expression was maximum at 2–5 h, and therefore, the 3-h induction time point was employed hereafter,

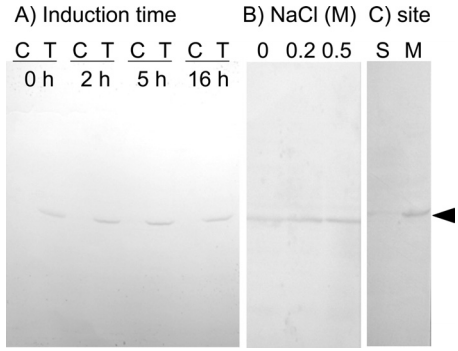

FIGURE 3. **Expression of $ApNa^+$-ATPase in *E. coli* DK8 cells.** *A*, effects of induction time. *B*, effects of NaCl. *C*, localization of $ApNa^+$-ATPase. *E. coli* DK8 cells were grown in the LB medium containing 1 mM isopropyl-β-D-thiogalactopyranoside. In *A*, the induction time was 0, 2, 5, and 16 h. *C* and *T* show the cells-expressing vector only and *$ApNa^+$-atp* operon, respectively. In *B*, LB medium contains 0.0, 0.2, and 0.5 M NaCl. In *C*, the $ApNa^+$-ATPase-expressing cells were fractionated as soluble (*S*) and membrane (*M*) fractions. The His tag-containing γ subunit (*arrowhead*) was detected by immunoblotting.

unless otherwise stated. The expression level of γ subunit increased with increase in NaCl concentrations (Fig. 3*B*). To examine the localization of γ subunit in DK8, *E. coli* cells expressing *$ApNa^+$-atp* were fractionated into the cytoplasmic, periplasmic, and membrane fractions, followed by SDS-PAGE and immunoblot analyses. The γ subunit was detected in the membrane fraction (Fig. 3*C*). These results suggest that the γ subunit and whole complex are assembled into the cytoplasmic membranes of *E. coli* cells.

As a next step, the *E. coli* membrane fraction was solubilized with Triton X-100, fractionated by 40–65% (g/v) ammonium sulfate, and applied to an ion exchange column chromatography. The active fractions were then used for activity measurements.

ATP Hydrolysis Activity in Inverted Membrane Vesicles of E. coli DK8 Cells—We next examined whether the expressed $ApNa^+$-ATPase has ATP hydrolysis activity. The ATP hydrolysis activity in the inverted membrane vesicles of $ApNa^+$-ATPase-expressing *E. coli* DK8 cells increased with increasing NaCl concentrations (Fig. 4*A*). The apparent K_m value for Na^+ was determined as 3.0 mM. The ATP hydrolysis activity of control cells (the empty vector transformants) was very low and did not increase upon the increase of NaCl concentration (data not shown). The ATP hydrolysis activity of $ApNa^+$-ATPase-expressing *E. coli* DK8 cells increased with increasing ATP (Fig. 4*B*); the apparent K_m value for ATP was determined to be 2.8 mM. The Na^+ content inside the $ApNa^+$-ATPase-expressing *E. coli* DK8 cells decreased when cells were transferred to a new Na^+-free medium, but no change in the Na^+ content was observed inside the control cells (data not shown). These results suggest that the *E. coli* DK8 cells expressing $ApNa^+$-ATPase can extrude Na^+ from inside the cells to the external medium.

Effect of Inhibitors on ATP Hydrolysis Activity in Inverted Membrane Vesicles of $ApNa^+$-ATPase-expressing E. coli DK8 Cells—The ATP hydrolysis activity in inverted membrane vesicles of $ApNa^+$-ATPase-expressing *E. coli* DK8 cells was strongly inhibited by azide (F_1 inhibitor; 55%), DCCD[2] (F_o

[2] The abbreviations used are: DCCD, *N*,*N*′-dicyclohexylcarbodiimide; CCCP, carbonyl cyanide *m*-chlorophenyl hydrazone.

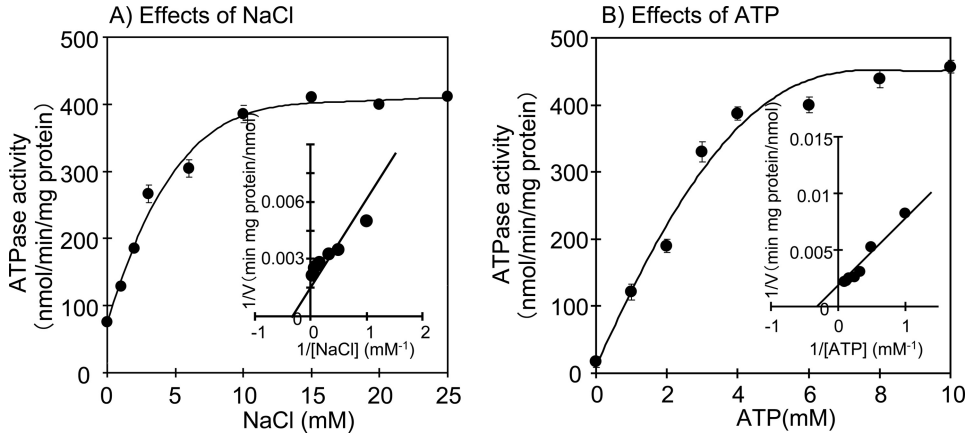

FIGURE 4. **Effects of NaCl (*A*) and ATP (*B*) on ATPase activity in inverted membrane vesicles of ApNa$^+$-ATPase-expressing *E. coli* DK8.** The ATPase activity was assayed by measuring the release of inorganic phosphate resulting from the hydrolysis of ATP. The reaction mixture (1 ml) contained 20 mM Tris-HCl, pH 7.6, 5 mM $MgCl_2$, membrane vesicles (30 μg protein), and various concentrations of NaCl. The reaction was started by addition of 4 mM ATP. All data are the average of three independent experiments with *error bars* representing S.E.

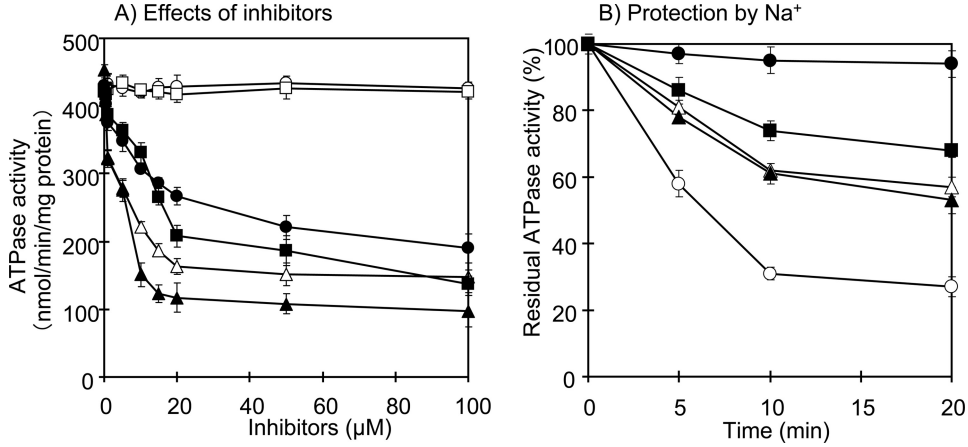

FIGURE 5. **Effects of inhibitors on ATPase activity in inverted membrane vesicles of *E. coli* DK8 expressing ApNa$^+$-ATPase and its protection by Na$^+$.** *A*, effects of inhibitors. *B*, effects of Na^+ on the inhibition by DCCD. In *A*, ATP hydrolytic activity was assayed in the presence of 10 mM NaCl, and each inhibitor was added to the reaction mixture 10 min before the start of the reaction: CCCP (○), KNO_3 (□), azide (●), DCCD (■), tributyltin chloride (▲), and monensin (△). In *B*, the inverted membrane vesicles was incubated with 200 μM DCCD in 20 mM Tricine-KOH, pH 9.0. The individual mixtures contained NaCl: 0 mM (○), 1 mM NaCl (▲), 10 mM NaCl (△), and 50 mM NaCl (■). One hundred percent activity corresponded to 423 nmol min^{-1} (mg protein)$^{-1}$. Also shown is the control without DCCD (●). Each value shows the average of three independent measurements.

inhibitor; 70%), tributyltin chloride (F_0 inhibitor; 80%), and monensin (Na^+-gradient dissipator; 70%), but not by CCCP (a protonophore) and KNO_3 (a permeant anion) (Fig. 5*A*). Moreover, Na^+ provided protection against inhibition by DCCD. When NaCl was added into the individual reaction medium, the DCCD-inhibited ATPase activity was decreased to 70, 40, and 30% in the presence of 1, 10, and 50 mM NaCl, respectively (Fig. 5*B*).

ATP Synthesis in Na$^+$-loaded Inverted Membrane Vesicles of E. coli DK8 Cells—To know whether the expressed ApNa$^+$-ATPase in DK8 cells has ATP synthesis activity, the ATP synthesis activity was assayed using the luciferin/luciferase reaction. The Na^+-loaded inverted membrane vesicles of *E. coli* DK8 cells were prepared and incubated with the reaction medium (0.5 ml) containing 5 mM potassium phosphate, pH 7.5, 5 mM $MgCl_2$, 0.2 M KCl, and 0.1 mM ADP. The ATP synthesis was observed in the membrane vesicles of ApNa$^+$-ATPase-expressing *E. coli* DK8 cells (Fig. 6*A*, *closed circles*), but not in the empty vector transformants (data not shown).

To examine the requirement of $\Delta\psi$ on ATP synthesis, inhibitors and ionophores were added to the reaction medium. Results showed that membrane potential-generating K^+/valinomycin and protonophore CCCP stimulated ATP synthesis (Fig. 6*A*), implying that ATP synthesis requires $\Delta\psi$ but not ΔpH. In contrast, the Na^+ gradient dissipator monensin and the F_0 inhibitor DCCD inhibited ATP synthesis, suggesting that ATP synthesis by F_1F_0-ATPase requires ΔpNa^+. Furthermore, application of external Na^+ (20 and 50 mM NaCl) into the reaction medium decreased the ATP synthesis (Fig. 6*B*). In other words, decrease in ΔpNa^+ due to external Na^+ causes decrease in the ATP synthesis.

Expression of ApNa$^+$-ATPase Confers Salt-stress Tolerance in E. coli—We next investigated the physiological role of ApNa$^+$-ATPase, namely the NaCl-stress tolerance in *E. coli*. As shown in Fig. 7, *E. coli* DK8 cells transformed with pTrcHis2C or pTrcHis2C-*ApNa$^+$-atp* exhibited similar growth patterns in the absence of NaCl. An increase in the NaCl concentration up to 0.2 and 0.5 M NaCl resulted in slow growth of all cells. How-

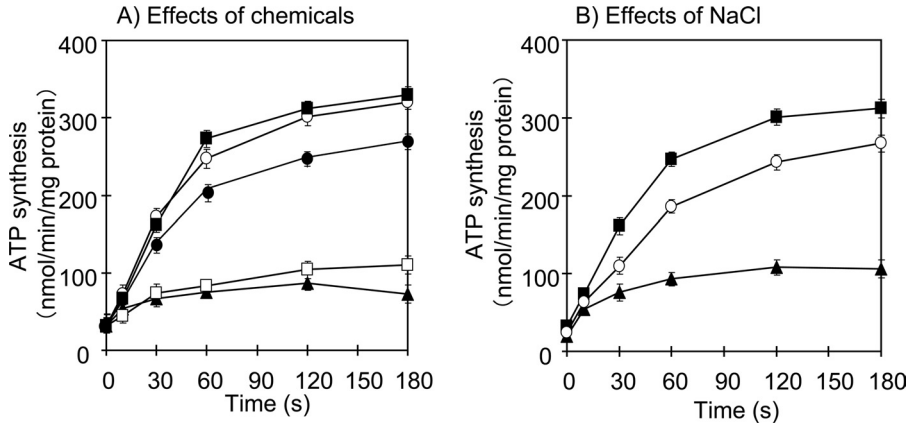

FIGURE 6. **ATP synthesis in Na$^+$-loaded inverted membrane vesicles of *E. coli* DK8.** *A*, effect of CCCP, DCCD, monensin, and valinomycin on the ATP synthesis in the Na$^+$-loaded inverted membrane vesicles of *E. coli* DK8 expressing ApNa$^+$-ATPase. ATP synthesis was measured in the reaction medium (0.5 ml) containing 5 mM potassium phosphate, pH 7.5, 5 mM $MgCl_2$, 0.2 M KCl, 0.1 mM ADP, and Na$^+$-loaded-membrane vesicles (30 μg protein) with or without addition of chemicals. Without chemical (●), 1 mM CCCP (■), 1 μM valinomycin (○), 100 μM DCCD (▲), and 10 μM monensin (□) in individual reaction. *B*, effect of external Na$^+$ on the ATP synthesis in the Na$^+$-loaded membrane vesicles of *E. coli* DK8 expressing ApNa$^+$-ATPase. ATP synthesis was measured in the presence of 1 μM valinomycin and various NaCl concentrations; 0 mM NaCl (■), 20 mM NaCl (○), and 50 mM NaCl (▲) in individual reaction.

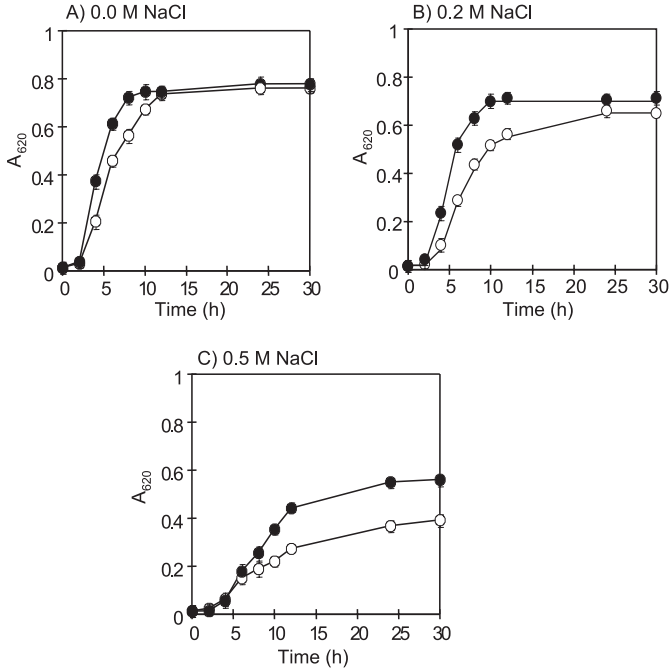

FIGURE 7. **Effects of NaCl on the growth of *E. coli* DK8 cells.** *E. coli* DK8 cells were grown in LB medium containing 0.0 M NaCl (*A*), 0.2 M NaCl (*B*), and 0.5 M NaCl (*C*). *Open circles* represent empty vector transformants, whereas *filled circles* represent ApNa$^+$-ATPase-expressing cells. Each value shows the average of three independent measurements.

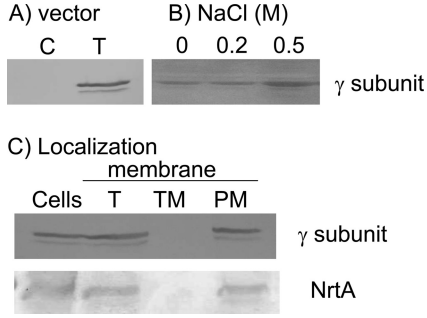

FIGURE 8. **Immunoblot analysis of ApNa$^+$-ATPase in the membrane vesicles of *Synechococcus* sp. PCC 7942 cells.** *A*, *Synechococcus* sp. PCC 7942 cells were transformed with vector (pUC303) (*C*) or pUC303-ApATPase (*T*). *B*, effect of NaCl on the expression of ApNa$^+$-ATPase in the ApNa$^+$-ATPase-expressing cells. The ApNa$^+$-ATPase-expressing cells were grown in the BG11 medium containing 0.0, 0.2, and 0.5 M NaCl. *C*, localization of ApNa$^+$-ATPase in *Synechococcus* sp. PCC 7942 cells. The ApNa$^+$-ATPase-expressing cells (*Cells*) were fractionated as total membrane vesicles (*T*), thylakoid membrane (*TM*), and plasma membrane (*PM*). The γ subunit of ApNa$^+$-ATPase and NrtA of nitrate transporter were detected by immunoblotting with anti-His tag and anti-NrtA (19) antibody, respectively.

ever, the growth rate of ApNa$^+$-ATPase-expressing cells was higher than that of empty vector transformants. Therefore, the effect of NaCl on growth of a salt-sensitive mutant *E. coli* TO114, in which *nhaA*, *nhaB*, and *chaA* genes were deleted, was determined. The *E. coli* TO114 cells transformed with pTrcHis2C-*ApNa$^+$-atp* grew in the growth medium containing 0.2 M NaCl, whereas the *E. coli* TO114 cells transformed with pTrcHis2C did not (data not shown). To determine whether *ApNa$^+$-atp* could complement *E. coli* DK8 (Δ*atp*), empty vector transformant and ApNa$^+$-ATPase-expressing cells were plated onto M13 minimal medium containing succinate as the sole carbon and energy source. Control plates contained glucose in the same amount as succinate. Results showed that empty vector transformants could grow only on glucose, whereas ApNa$^+$-ATPase-expressing cells could grow on both glucose and succinate (data not shown). Hence, the *ApNa$^+$-atp* operon encoding F_1F_0-ATPase was able to produce ATPase in the host cells, supporting the growth of *E. coli* DK8 on a non-fermentable carbon source.

Expression of ApNa$^+$-atp Operon in the Freshwater Cyanobacterium Synechococcus sp. PCC 7942—The expression plasmid pUC303-*ApNa$^+$-atp* containing isopropyl-β-D-thiogalactopyranoside-inducible *trc* promoter was introduced into *Synechococcus* sp. strain PCC 7942 cells. The expression of γ subunit of ApNa$^+$-ATPase was detected in the membrane vesicles of ApNa$^+$-ATPase-expressing cells (Fig. 8*A*). Its expression level increased with the increase of NaCl in the growth medium (Fig. 8*B*). To examine the localization of ApNa$^+$-ATPase, total membrane fractions were applied on the sucrose density gradient as described in "Experimental Procedures" (14). Thylakoid membranes contained ~4.1 μg chlorophyll per

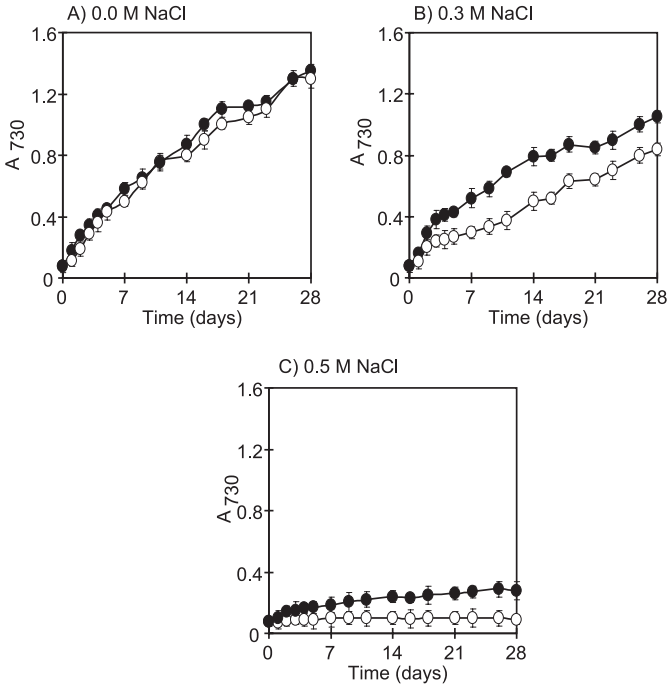

FIGURE 9. **Effects of NaCl on the growth of *Synechococcus* sp. PCC 7942 cells.** *Synechococcus* sp. PCC 7942 cells were grown in the BG11 medium containing 0.0 M NaCl (*A*), 0.3 M NaCl (*B*), and 0.5 M NaCl (*C*). *Open circles* represent the empty vector transformants, whereas *filled circles* represent the $ApNa^+$-ATPase-expressing cells. Each value shows the average of three independent measurements.

mg protein, whereas cytoplasmic membranes were essentially free of chlorophyll (data not shown). Moreover, data presented in Fig. 8*C* revealed that a single protein band of the corresponding molecular mass of γ subunit of $ApNa^+$-ATPase was found in plasma membrane fraction, which was identified by the presence of the nitrate transporter NrtA (19). This indicated that $ApNa^+$-ATPase was localized in the plasma membrane of $ApNa^+$-ATPase-expressing cells.

It was shown that all of the transformants could grow at almost the same rate in the BG11 medium (Fig. 9*A*). At 0.3 M NaCl concentration, the growth rate of both empty vector transformants and $ApNa^+$-ATPase-expressing cells decreased but the growth rate of $ApNa^+$-ATPase-expressing cells is higher than the growth rate of empty vector transformants (Fig. 9*B*). At 0.5 M NaCl concentration, empty vector transformants could not grow, whereas $ApNa^+$-ATPase-expressing cells could (Fig. 9*C*), indicating that the *$ApNa^+$-atp* transformation impaired growth at high salinity.

DISCUSSION

The sequence of *$ApNa^+$-atp* operon was obtained from the shotgun genome sequencing of *A. halophytica*. Nine ORFs were organized in the order *atpD* (β), *atpC* (ϵ), *atpI* (I), hypothetical gene (*hyp*), *atpB* (a), *atpE* (c), *atpF* (b), *atpA* (α), *and atpG* (γ) (Fig. 1), which is different from other bacteria. In *C. paradoxum, E. coli*, *I. tartaricus,* and *P. modestum*, the *atp* operon consists of nine structural genes, *atpI* (I), *atpB* (a), *atpE* (c), *atpF* (b), *atpH* (δ), *atpA* (α), *atpG* (γ), *atpD* (β), and *atpC* (ϵ), which are grouped together to form a single transcriptional unit (16–18, 20, 21). The *atp* operon in a strictly anaerobic *A. woodii* consists of 11 genes, including nine genes found in the bacterial *atp* operons and additional two copies of *atpE* (c) (22). In addition, the structural genes in cyanobacteria *Anabaena* strain PCC 7210, *Synechococcus* strain PCC 6301, and *Synechocystis* sp. PCC 6803 are organized in two separate domains, with one containing *atpB* (a), *atpE* (c), *atpF* (b), *atpH* (δ), *atpA* (α), and *atpG* (γ), whereas the other contained *atpD* (β) and *atpC* (ϵ) (23–25). Although the deduced protein sequences of nine $ApNa^+$-ATPase subunits showed low percent identity compared with the corresponding sequences of F-type ATPase subunits from different species, the conserved amino acids Ser^{68} and Thr^{69} at the Na^+-binding site of the $ApNa^+$-ATPase subunit c were found (supplemental Fig. S1). The Na^+-binding site of the *I. tartaricus* ATPase and H^+-binding site of the spinach chloroplast ATPase subunit c were compared (2). Alanine was present at position 62 of the H^+-translocating ATPase, whereas a polar serine or threonine was observed in the equivalent position of Na^+-translocating ATPase. Likewise, the hydrophobic side chain leucine was found in H^+-translocating ATPase at position 63, but threonine was found at the equivalent position of Na^+-translocating ATPase. The data presented above clearly indicate that F-typeNa^+-ATPase from *A. halophytica* is a Na^+-translocating ATPase.

Furthermore, this study examined the biochemical properties and physiological functions of $ApNa^+$-ATPase. The expression of $ApNa^+$-ATPase in $ApNa^+$-ATPase-expressing cells could impair its growth under high salinity (Fig. 7). The ATP hydolysis activity in inverted membrane vesicles of $ApNa^+$-ATPase-expressing *E. coli* DK8 was dependent on NaCl and ATP concentration in the reaction medium (Fig. 4). Moreover, the Na^+ extrusion from Na^+-loaded $ApNa^+$-ATPase-expressing cells was observed after the cells were energized with glucose (data not shown), suggesting that the Na^+ extrusion is likely due to the contribution by $ApNa^+$-ATPase because glucose can yield ATP during its metabolism. $ApNa^+$-ATPase was confirmed as a member of F-type Na^+-ATPase by using appropriate inhibitors. The ATPase activity was inhibited by azide (F_1 inhibitor), DCCD (F_0 inhibitor), or tributyltin chloride (F_0 inhibitor). In addition, it was found that monensin (Na^+-gradient dissipator) inhibited ATPase activity, whereas CCCP (a protonophore) and KNO_3 (a permeant anion) did not inhibit activity (Fig. 5*A*). These data indicate the involvement of ΔpNa^+ but not ΔpH on ATP hydrolysis. Furthermore, it was found that Na^+ could protect ATPase activity from DCCD inhibition in a pH-dependent manner (Fig. 5*B*). Using another approach, ATP synthesis was observed in the Na^+-loaded membrane vesicles of $ApNa^+$-ATPase-expressing *E. coli* DK8 cells in the presence of ΔpNa^+ and $\Delta\psi$ (Fig. 6). Our data revealed that ATP synthesis was stimulated in the presence of K^+/valinomycin. ATP synthesis decreased when external Na^+ and monensin (Na^+ gradient dissipator) were added because both of them reduced ΔpNa^+ (Fig. 6*B*). Based on these results, it can be concluded that ATP synthesis catalyzed by $ApNa^+$-ATPase requires ΔpNa^+.

As per the above data, we thought that the introduction of *$ApNa^+$-atp* operon into the freshwater cyanobacterium *Synechococcus* sp. PCC 7942 will confer salt tolerance to this organism. As expected, the $ApNa^+$-ATPase-expressing cells could

grow in the BG11 medium containing 0.5 M NaCl, whereas the empty vector transformants could not (Fig. 9). From these results, *$ApNa^+$-atp* transformation could improve salt tolerance in the freshwater cyanobacterium *Synechococcus* sp. PCC 7942 as well as *E. coli* DK8 mutant (Δ*atp*) and salt-sensitive mutant *E. coli* TO114. Western blot analysis revealed that the expression level of γ subunit of $ApNa^+$-ATPase increased with increasing NaCl concentration in the growth medium (Fig. 8*B*). Taken together, our results strongly suggest a role for $ApNa^+$-ATPase in the salt-stress tolerance of this photosynthetic organism.

Acknowledgment—We thank Professor T. Omata (Nagoya University) for the generous gift of the nitrate transporter antibody.

REFERENCES

1. von Ballmoos, C., Wiedenmann, A., and Dimroth, P. (2009) *Annu. Rev. Biochem.* **78,** 649–672
2. Vollmar, M., Schlieper, D., Winn, M., Büchner, C., and Groth, G. (2009) *J. Biol. Chem.* **284,** 18228–18235
3. Beyenbach, K. W., and Wieczorek, H. (2006) *J. Exp. Biol.* **209,** 577–589
4. Zhu, J. K. (2003) *Curr. Opin. Plant Biol.* **6,** 441–445
5. Shono, M., Hara, Y., Wada, M., and Fujii, T. (1996) *Plant Cell Physiol.* **37,** 385–388
6. Balnokin, Y. V., and Popova, L. G. (1994) *FEBS Lett.* **343,** 61–64
7. Waditee, R., Hibino, T., Tanaka, Y., Nakamura, T., Incharoensakdi, A., and Takabe, T. (2001) *J. Biol. Chem.* **276,** 36931–36938
8. Waditee, R., Tanaka, Y., Aoki, K., Hibino, T., Jikuya, H., Takano, J., Takabe, T., and Takabe, T. (2003) *J. Biol. Chem.* **278,** 4932–4942
9. Wutipraditkul, N., Waditee, R., Incharoensakdi, A., Hibino, T., Tanaka, Y., Nakamura, T., Shikata, M., Takabe, T., and Takabe, T. (2005) *Appl. Environ. Microbiol.* **71,** 4176–4184
10. Waditee, R., Hibino, T., Nakamura, T., Incharoensakdi, A., and Takabe, T. (2002) *Proc. Natl. Acad. Sci. U.S.A.* **99,** 4109–4114
11. Fukaya, F., Promden, W., Hibino, T., Tanaka, Y., Nakamura, T., and Takabe, T. (2009) *Appl. Environ. Microbiol.* **75,** 6626–6629
12. Waditee, R., Hossain, G. S., Tanaka, Y., Nakamura, T., Shikata, M., Takano, J., Takabe, T., and Takabe, T. (2004) *J. Biol. Chem.* **279,** 4330–4338
13. Moriyama, Y., Iwamoto, A., Hanada, H., Maeda, M., and Futai, M. (1991) *J. Biol. Chem. 266,* 22141–22146
14. Berger, S., Ellersiek, U., and Steinmüller, K. (1991) *FEBS Lett.* **286,** 129–132
15. Waditee, R., Bhuiyan, N. H., Hirata, E., Hibino, T., Tanaka, Y., Shikata, M., and Takabe, T. (2007) *J. Biol. Chem.* **282,** 34185–34193
16. Walker, J. E., Saraste, M., Runswick, M. J., and Gay, N. J. (1982) *EMBO J.* **1,** 945–951
17. Meier, T., von Ballmoos, C., Neumann, S., and Kaim, G. (2003) *Biochim. Biophys. Acta* **1625,** 221–226
18. Miki, J., Maeda, M., Mukohata Y., and Futai, M. (1988) *FEBS Lett.* **232,** 221–226
19. Omata, T. (1995) *Plant Cell Physiol.* **36,** 207–213
20. Ferguson, S. A., Keis, S., and Cook, G. M. (2006) *J. Bacteriol.* **188,** 5045–5054
21. Kaim, G., Ludwig, W., Dimroth, P., and Schleifer, K. H. (1992) *Eur. J. Biochem.* **207,** 463–470
22. Rahlfs, S., Aufurth, S., and Müller, V. (1999) *J. Biol. Chem.* **274,** 33999–34004
23. Curtis, S. E. (1987) *J. Bacteriol.* **169,** 80–86
24. Cozens, A. L., and Walker, J. E. (1987) *J. Mol. Biol.* **194,** 359–383
25. Lill, H., and Nelson, N. (1991) *Plant. Mol. Biol.* **17,** 641–652